Optimizing mechanical properties of AA7075 Metal Matrix Composites reinforced with TiB_2 and ZrO_2 particulates

Nagaraj S. Dhongade
School of Mechanical Engineering, KLE Technological University, Hubballi, India
nagaraj.dhongade@gmail.com

Vinod Kumar V. Meti
Department of Automation & Robotics, KLE Technological University, Hubballi, India
vinod_meti@kletech.ac.in, https://orcid.org/0000-0001-5692-9693

I. G. Siddhalingeshwar, G. U. Raju*
School of Mechanical Engineering, KLE Technological University, Hubballi, India
igs@kletech.ac.in, https://orcid.org/0000-0002-2361-596X
raju_gu@kletech.ac.in, https://orcid.org/0000-0003-0234-1055

M. A. Umarfarooq*
Department of Mechanical Engineering, Karpagam Academy of Higher Education, Coimbatore, Tamil Nadu, India.
Center for Material Science, Department of Mechanical Engineering, Karpagam Academy of Higher Education, Coimbatore, Tamil Nadu, India.
umarfarooq.ma@gmail.com, https://orcid.org/0000-0002-9369-7913

N.R. Banapurmath, Ashok M. Sajjan
Centre of Excellence in Material Science, School of Mechanical Engineering, KLE Technological University, Hubballi-580031, India
nr_banapurmath@kletech.ac.in, https://orcid.org/0000-0002-1280-6234
am_sajjan@kletech.ac.in, https://orcid.org/0000-0003-1251-8803

Vinayak S. Uppin
Department of Mechanical Engineering, SDM College of Engineering & Technology, Dharwad, Visvesvaraya Technological University, Belagavi, Karnataka, India
ursuppin@gmail.com, https://orcid.org/0000-0001-9093-2757

Balbir Singh
Department of Aeronautical and Automobile Engineering, Manipal Institute of Technology, Manipal Academy of Higher Education (MAHE), Manipal, Karnataka, India
balbir.s@manipal.edu, https://orcid.org/0000-0001-9591-3694

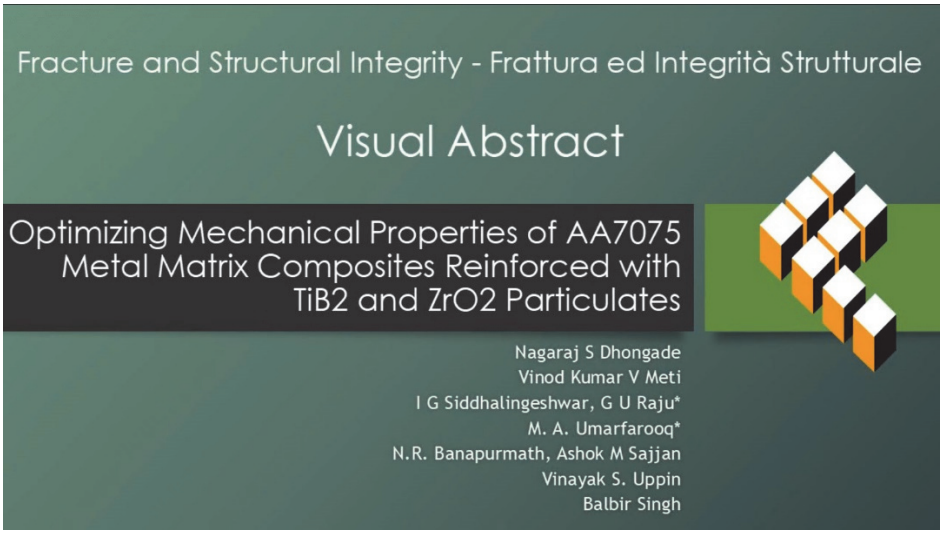

Citation: Dhongade, N. S., Meti, V. K., Siddhalingeshwar, I. G., Raju, G. U., Umarfaroq, M. A., Banapurmath, N. R. Sajjam, A. M. Uppin, V. S., Singh, B., Optimizing mechanical properties of AA7075 Metal Matrix Composites reinforced with TiB_2 and ZrO_2 particulates, Fracture and Structural Integrity, 74 (2025) 1 -19.

Received: 22.05.2025
Accepted: 26.06.2025
Published: 03.07.2025
Issue: 10.2025

KEYWORDS. Metal matrix Hybrid composites, Stir casting, Microstructural analysis, Mechanical properties, Tribological properties.

INTRODUCTION

Advancements in the material properties of defense, aerospace, automobile, aviation, marine, and structural industries are the current fields of interest for many researchers and scientists across the globe . Davis *et al.* [1] briefs about aluminum and its properties. All types of aluminum alloys (cast and wrought alloys) have been discussed in this paper by stating their chemical composition, mechanical properties, and applications. Advanced materials refer to those with enhanced properties that out-master the properties of the present materials. Aluminum is widely known and used for its properties, which include good formability, corrosion resistance, high electrical and thermal conductivity, good finish ability, and non-pyrophoric [2-3].

Aluminum alloys or aluminum matrix composites (AMCs) have a phenomenally high strength-to-weight ratio, opening doors for various engineering applications. Due to its solid mechanical qualities, AA7075, having zinc as the primary alloying element, is employed in multiple industries, including aerospace, automotive, marine, and structural applications. Wallace and Beddoes [2] employed transmission electron microscopy to assess a heat-treatment procedure that enhances stress-corrosion cracking resistance without losing yield strength in AA7075. According to the findings, heat treatment (as retrogression and re-aging) results in enormous grain-boundary and coherent matrix precipitates. AMCs enhance the base metal's properties by adding reinforcements of different compositions. AMCs have good thermal conductivity and machinability and accept all manufacturing techniques.

When added to matrix material as reinforcement, ceramics improve the tribological and mechanical properties according to their compositions. Ceramics are well known for their high creep resistance and have boiling points ranging from 1000 ^{o}C to 3000 ^{o}C. Ceramic reinforcements are classified into oxides, nitrides, borides, and carbides. Researchers have reported that TiB_2 and ZrO_2 ceramic particles improve the mechanical and tribological properties such as modulus, creep resistance, wear resistance, fatigue properties, hardness, and yield strength of the base metal matrix [3]. Titanium boride (TiB_2) is known for its strength, chemical inertness, and wear-resisting properties. It has a density of 4.52 g/cm^3. Due to its high hardness, it opens applications for ballistic armor, composite materials, and various cutting tools. It exhibits a melting point of 2970 °C and a hardness of 1800 HV. Meti *et al.* [4] stated the importance of TiB_2 reinforcement particles in the AA7075 matrix processed through ultrasound casting. By reinforcing TiB_2 particles, the hardness and wear resistance of the matrix were increased. Further, treating the composite with an ultrasound technique increased the mechanical and tribological properties due to refinement in the grain structure and uniform distribution of particles in the metal matrix [5]. Rajan *et al.* [6] synthesized the AA7075/TiB_2 composite using an in-situ salt-melt reaction technique. TiB_2 reinforcement particles were synthesized using K_2TiF_6 and KBF_4 salts. SEM micrographs indicated a homogeneous distribution of reinforcing particles

with a muscular bonding strength and a distinct interface. The addition of TiB_2 reinforcement particles improved the mechanical behaviour of the AA7075/TiB_2 composite.

Zirconium dioxide (zirconia: ZrO_2) ceramic powder is generally used in dental applications. Unlike other ceramics, zirconia has a high hardness, which makes it brittle. Zirconia possesses high strength, fracture toughness, and wear resistance and can hold high temperatures up to 2400 °C. Zirconia is known as 'ceramic steel' as its modulus of elasticity is similar to steel. In a related study, Reddy et al. [7] investigated the effect of varying ZrO_2 concentrations on the mechanical and wear behavior of AA7075-based composites. Their scanning electron microscopy (SEM) analysis confirmed a homogeneous distribution of reinforcement particles throughout the matrix. The results revealed notable improvements in both tensile strength and surface hardness, with the AA7075/1.5 wt% ZrO_2 composite exhibiting optimal performance metrics among the compositions studied.

Hybrid composites are in high demand worldwide due to the wide range of emerging applications in engineering. The market is for new-generation material, which holds a high strength-to-weight ratio. Hybrid metal matrix composites (HMMCs) are advanced engineered materials composed of two or more distinct reinforcements i.e. metallic, ceramic, or non-metallic which arestrategically integrated within a metal matrix to achieve synergistic improvements in performance. As highlighted by Zhou et al. [8], HMMCs demonstrate superior mechanical robustness and tribological resilience compared to their monolithic or single-reinforcement counterparts. The study also provides a comparative overview of fabrication techniques,such as stir casting, powder metallurgy, and squeeze casting specificallyemployed in synthesizing hybrid MMCs, each influencing the composite's microstructure and resultant properties. Moreover, the inclusion of diverse reinforcements has been shown to significantly impact mechanical strength, electrical conductivity, and thermal stability. Owing to this multi-functional enhancement, hybrid MMCs are increasingly considered promising alternatives to conventional composites for demanding applications across aerospace, automotive, and electronic sectors. Hybrid composites are in high demand worldwide due to wide branches emerging applications in engineering. One of the most important requirements for engineering applications is high creep resistance, which is not satisfied by an alloy. Composites can stabilize this drawback. Because of their high strength, stiffness, low weight, and creep resistance, composites can be used in a variety of applications, including defense, aerospace, marine, and structural applications. Aluminum hybrid composites are prominent in these applications as they are highly efficient, low-cost, and easy to adapt to various manufacturing techniques.

Manufacturing techniques used to fabricate any composite plays an essential role in determining the final properties of the composites. There are different ways to process AMCs, such as liquid, solid, and deposition. Research denotes that liquid-state and solid-state processing are extensively used for manufacturing AMCs. Stir casting is designated as the most economical method to fabricate AMCs. Here, the reinforcements are directly introduced into the molten metal. The major challenge in stir casting is that the reinforcement particles tend to sink due to their density relative to the molten metal [8-9]. According to Kumar et al. [9], the stir casting process remains the most cost-effective and scalable technique for fabricating metal matrix composites (MMCs), particularly advantageous for large-scale industrial production. Aluminum matrix composites (AMCs), owing to their exceptional mechanical strength and superior wear resistance, have garnered significant interest in high-performance structural applications. The authors emphasized that stir casting promotes uniform dispersion of reinforcement particulates within the matrix, enhances wettability between the matrix and reinforcements, and effectively minimizes porosity—thereby contributing to improved interfacial bonding and overall composite integrity. Meti *et al.* [7] suggested different processing techniques to develop AMCs. AMCs containing different compositions of reinforcements showed better results using liquid-state techniques. Good bonding and straightforward interface with uniform distribution of reinforcements were seen through liquid state techniques. Further, when treating the composite with the ultrasound technique, there was an enhancement in the mechanical and tribological characteristics of the matrix material. They stated that ductility and wear rate decrease as the fraction of reinforcements increases. Prakash and Binay Kumar [10] conducted a comprehensive investigation into the influence of zirconium diboride (ZrB_2) at varying concentrations (1–5 wt.%) combined with 2 wt.% fly ash on the mechanical and tribological performance of AA7075-based hybrid metal matrix composites (HMMCs) subjected to T6 heat treatment. Their findings revealed that the composite reinforced with 5 wt.% ZrB_2 exhibited a remarkable enhancement in tensile strength and hardness, recording improvements of up to 77% and 15%, respectively, when benchmarked against the unreinforced AA7075 alloy. Additionally, under a 40 N load condition, the same composite demonstrated a significant 46.94% reduction in specific wear rate and a noticeable decrease in the coefficient of friction. These enhancements are attributed to the synergistic effect of hard ceramic reinforcements and the optimized microstructural characteristics induced by the heat treatment process.

This study is primarily focused on the fabrication of hybrid aluminum matrix composites (AMCs) reinforced with titanium diboride (TiB_2) and zirconium dioxide (ZrO_2) particulates, aiming to elucidate the interfacial interactions between the ceramic reinforcements and the aluminum matrix. The investigation systematically evaluates the mechanical and tribological performance of hybrid composites with varying reinforcement compositions. Addressing common limitations of

conventional composites, this work targets enhancements in toughness, fatigue resistance, corrosion stability, and manufacturability, while enabling tailored property combinations that surpass those achievable by monolithic metals, ceramics, or polymers. The specific objectives include: (1) synthesizing TiB_2 and ZrO_2-reinforced hybrid AMCs via controlled processing techniques; (2) comprehensive evaluation of their mechanical properties—including tensile strength, hardness, and wear resistance; and (3) detailed microstructural characterization to correlate reinforcement distribution and morphology with the observed performance across different composite formulations.

One of the most important aspects of this paper is its amendment made when compared to the existing research by the authors, reference [17]. The work here introduces several key amendments compared to the previous version [17], reflecting a shift in focus and enhancement in technical detail. One of the most notable changes is the emphasis on the stir casting process as the primary fabrication method for the hybrid metal matrix composites (HMMCs) in detail here, whereas the previous combined stir casting with hot forging and highlighted the microstructural refinement resulting from the forging process. The forging step and its associated grain refinement benefits have been omitted in the new version, signaling a methodological simplification and redirection of the study. Another important amendment is the expansion of the reinforcement composition range. While the previous work [17] investigated TiB_2 at a constant 5 wt% and ZrO_2 at 4 wt% and 6 wt%, the revised version here broadens this scope by including a lower ZrO_2 concentration of 2 wt%, offering a more comprehensive evaluation of reinforcement variation and its effects on composite properties. The new work here also incorporates quantitative mechanical and wear performance data, which was absent in the earlier version. Specific values are reported for hardness, which increased from 55 Hv to 102.40 Hv (an 85.45% improvement), and yield strength, which rose from 107 MPa to 123 MPa (a 15% increase). Furthermore, the wear rate of the composites is now explicitly measured (155 μm at 10N load), and a wear mechanism is proposed, stating that the ceramic reinforcements serve as lubricating agents that reduce direct contact between the matrix and the counterface during sliding. This level of analytical depth was not presented in the previous version. In addition to SEM microstructural analysis, the revised version also highlights the EDX elemental mapping of the optimal AA7075/5%TiB_2/4%ZrO_2 composition, which confirms the uniform spatial distribution of aluminum, zinc, titanium, boron, and zirconium elements. This mapping validates the successful dispersion of the reinforcement particles within the matrix and supports the observed improvements in mechanical and tribological properties by ensuring consistent phase interaction and load transfer across the composite structure. There is also refinement of the identification of the best-performing composition with more robust justification based on performance metrics.

DETAILED METHODOLOGY

In this study, AA7075 was utilized as the matrix material, with its chemical composition detailed in Tab. 1. TiB_2 and ZrO_2 Reinforcements were taken according to the design required (TiB_2) was fixed for 5% in every iteration and ZrO_2 with variable composition, i.e., 2%, 4%, and 6%). According to the below-mentioned calculations, a fixed amount of aluminum alloy 7075 (i.e., 300 gms) was taken in the crucible.

Dimensions of iron mould: length = 170mm, Thickness = 6 mm, Width = 80 mm

$$\text{Density} = \text{Mass} / \text{Volume} \quad (1)$$

Density of AA7075 = 2.81 g/cm^3, Volume of the mould = 170 * 80 * 6 mm

Using Eqn. 1 → 2.81 g/cm^3 = M (gm) / [170 * 80 * 6] (mm)

M = 230 gm ≈ 250 gm

- For AA7075 / 5% TiB_2 / 2% ZrO_2

TiB_2 = 250*0.05 = 12.5 gm

ZrO_2 = 250*0.02 = 5 gm

- For AA7075 / 5% TiB_2 / 4% ZrO_2

TiB_2 = 250*0.05 = 12.5 gm

ZrO_2 = 250*0.04 = 10 gm

- For AA7075 / 5% TiB_2 / 6% ZrO_2

TiB_2 = 250*0.05 = 12.5 gm

ZrO_2 = 250*0.06 = 15 gm

The stir casting technique used a vertical muffle furnace (Power: 3KW, Voltage: 230V, Max Temperature: 1200 °C). AA7075 was heated to 800°C [11]. The calculated amount of reinforcements was added to the molten metal and continuous stirring

every 10 minutes 5 times using a graphite rod to attain homogeneity and reduce the possibility of agglomeration. The synthesis of AA7075/TiB_2/ZrO_2 composite using in-situ casting is illustrated in Fig. 1. Hexachloroethane (C_2Cl_6) was added for the degasification process, which removes the trapped air from the melt and enhances the properties of the composite.

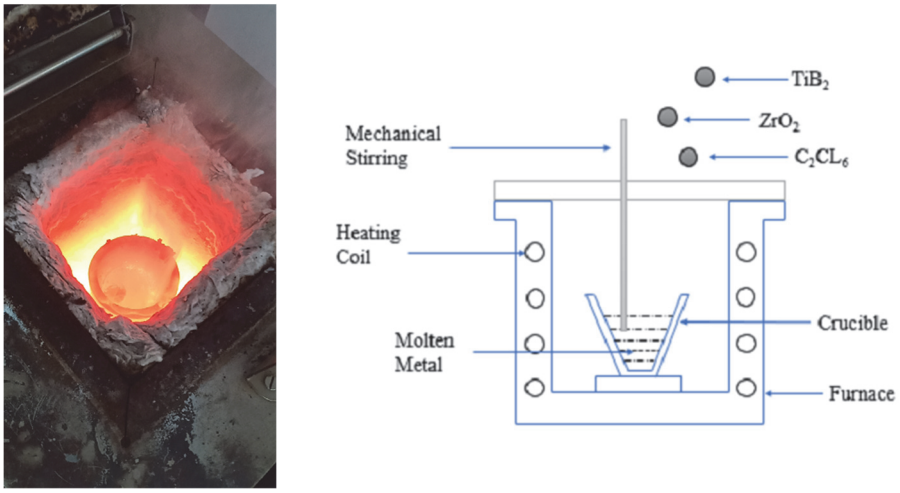

Figure 1: Schematic representation of Hybrid AMC utilizing situ casting.

Zn	Mg	Cu	Fe	Cr	Si	Mn	Ti	Ni	Al
5.60	2.60	1.60	0.30	0.25	0.30	0.20	0.20	0.02	Bal

Table 1: AA7075 chemical composition (wt.%).

Zirconia paste was applied to the mold. Zircon's low wettability allows high precision casting with a good surface finish. It also prevents the melt from sticking to the die and avoids metal penetration into the mold. The melt was poured using the crucible tongs into the pre-heated iron mold and allowed to solidify. Pre-heating of the mold is required for the uniform distribution of the molten melt. After the fabrication, the hybrid composite was subjected to different machining processes to prepare specimens for various testing. Specimens were prepared for microstructural studies, hardness tests, tensile tests, and wear tests according to ASTM standards. It is schematically shown in Figs. 2 and 3.

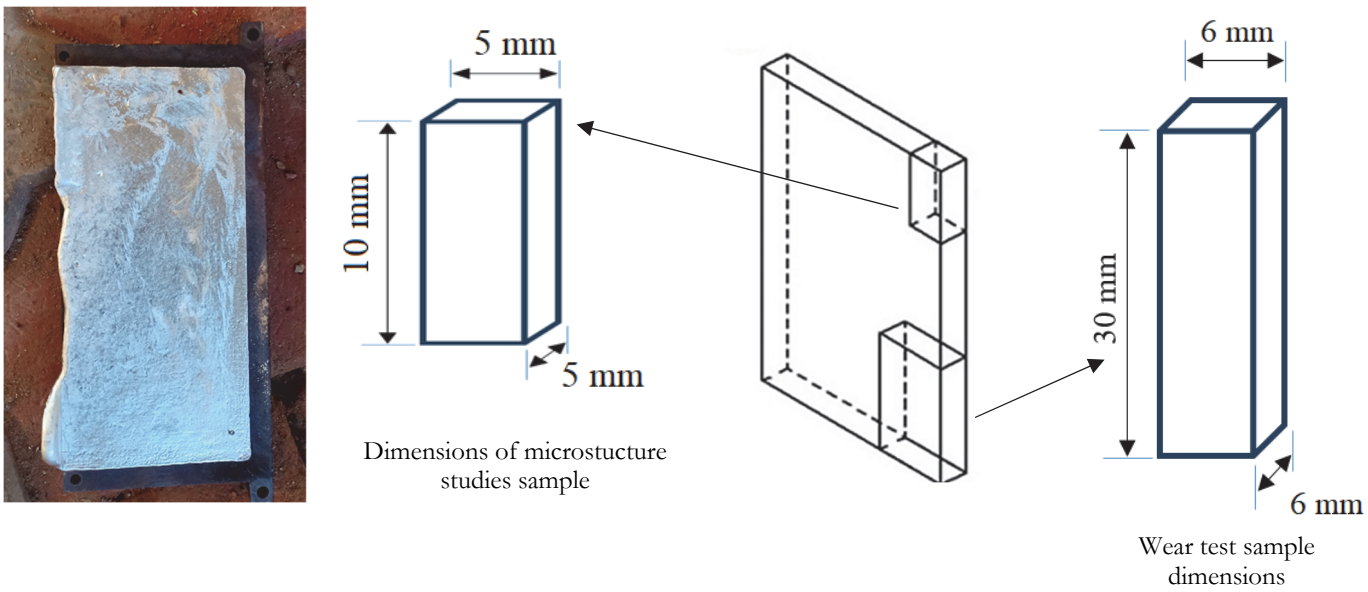

Figure 2: Casted Hybrid MMC with Schematic illustration for specimen.

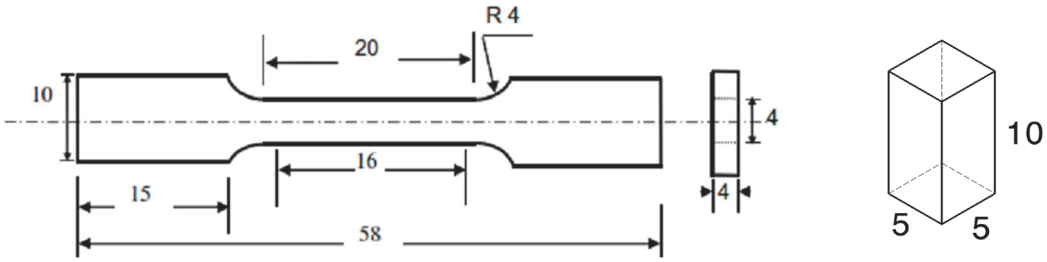

Figure 3: Schematic illustration for tensile test and hardness test specimen.

Microstructural characterization was conducted employing a high-resolution field emission scanning electron microscope (FE-SEM, ThermoFisher Apreo 2S HiVac, USA) following the guidelines stipulated in ASTM E3. This analysis facilitated an in-depth examination of grain morphology, grain boundary delineation, and the spatial distribution and homogeneity of reinforcement particulates within the aluminum matrix composite. A specimen with a dimension of 10×5×5 was cut out from the cast metal using a hexa-blade. Further, the model's surface was polished using SiC (emery paper), having grit sizes 80, 120, 400, 1000, and 1200.

Specimens were further polished to mirror finish using a polishing machine (Bainpol Metco, Chennai - India) shown in Fig. 4 containing velvet cloth (lapping cloth), smeared with 1-0.5 μm diamond paste. Metallographic specimens of the hybrid composites were chemically etched using Keller's reagent, composed of 2.5% nitric acid (HNO_3), 1.5% hydrochloric acid (HCl), 1% hydrofluoric acid (HF), and 95% deionized water, for a controlled duration of 30 seconds. This etching protocol effectively revealed well-defined grain boundaries and microstructural features, which were subsequently examined in detail via high-resolution scanning electron microscopy (SEM) to elucidate the reinforcement morphology and matrix–reinforcement interfacial characteristics.

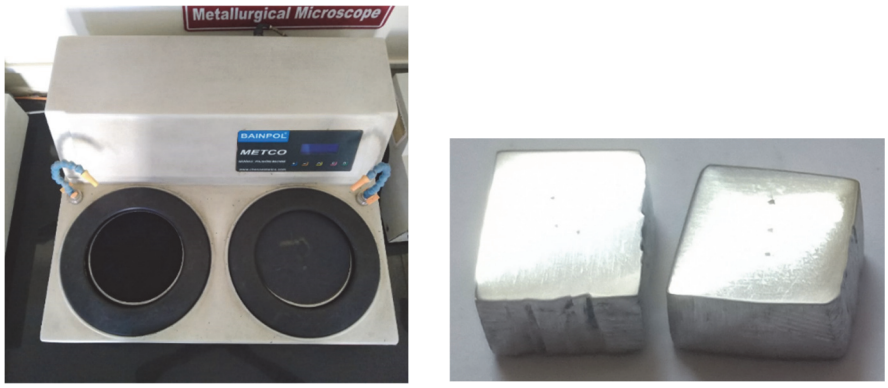

Figure 4: Grinding/Polishing machine and SEM specimen.

Fig. 5 depicts the optical micrograph of the dendritic samples captured with 100x magnification. The hardness evaluation of the AA7075/TiB_2/ZrO_2 hybrid composites was conducted in accordance with the ASTM E92 utilizing a Vickers microhardness tester (Fuel Instruments and Engineers Pvt. Ltd., India), as depicted in Fig. 6. This standardized testing protocol ensured precise quantification of the composite's resistance to localized plastic deformation, facilitating reliable assessment of the reinforcement effects on matrix hardness. Specimens (10×5×5 mm) were placed, and an indentation was made using a diamond indenter. Each indentation was made for 10 sec with a load of 10 kgf. After the indentation, the average diagonal length was examined and noted down. Further, the Vickers hardness number (H_v) was determined using the formula:

$$H_v = 1.854\frac{P}{d^2}$$

where 'P' = Indentation load (kgf) and 'd' = Mean diagonal length (mm)

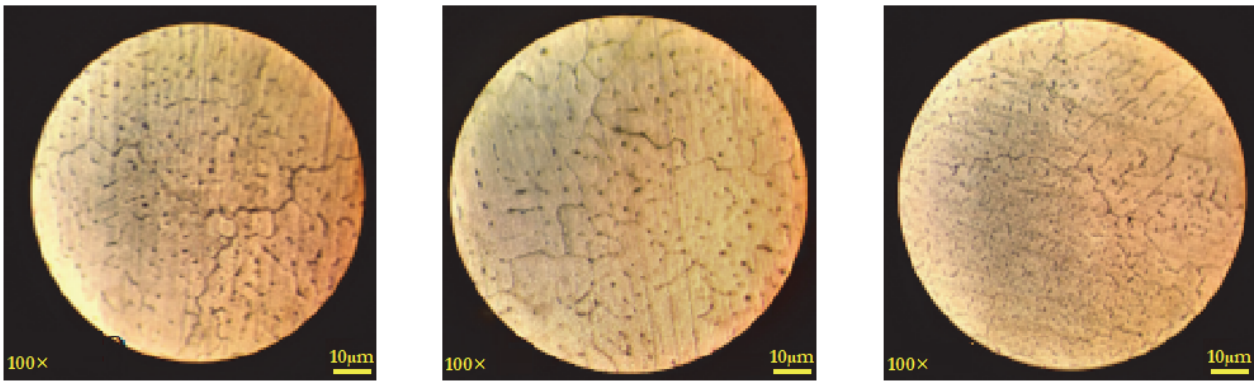

Figure 5: Optical micrographs illustrating the microstructural morphology of hybrid composites with 100x magnification: (a) AA7075 reinforced with 5 wt.% TiB_2 and 2 wt.% ZrO_2, (b) AA7075 reinforced with 5 wt.% TiB_2 and 4 wt.% ZrO_2, and (c) AA7075 reinforced with 5 wt.% TiB_2 and 6 wt.% ZrO_2, revealing characteristic dendritic architectures and reinforcement distribution within the aluminum matrix.

Figure 6: Vickers hardness tester and Hardness specimen.

Tensile test specimens were meticulously fabricated following the ASTM E8M standard, featuring a gauge length of 16 mm and a thickness of 4 mm, as illustrated in Fig. 7. The specimens were precision-machined from the cast hybrid composite using CNC milling to ensure dimensional accuracy. The geometric design maintained a gauge length to the square root of cross-sectional area ratio within the optimal range of 4 to 4.5, where L_0 denotes the gauge length and A_0 represents the initial cross-sectional area. Mechanical characterization was conducted on a micro universal testing machine (Mecmesin Multitest 10-i, UK), specifically engineered for low-force microstructural evaluation under ambient conditions. Testing proceeded at a controlled crosshead displacement rate of 0.3 mm/min until specimen failure, with real-time acquisition of load and displacement data. Subsequently, engineering stress–strain curves were generated to analyze the mechanical response and deformation behavior of the composites.

Figure 7: Tensile specimen

Dry sliding wear and frictional behavior of the hybrid composites were systematically evaluated using a pin-on-disc tribometer (DUCOM, India) in accordance with the ASTM G99, as depicted in Fig. 8. Test specimens, machined to dimensions of 30 × 5 × 5 mm, served as pins and were slid against an EN-32 hardened steel disc with a hardness of 62 HRC. The disc maintained a constant peripheral velocity of 1.5 m/s with a fixed rolling diameter of 100 mm. Wear tests were conducted under variable normal loads of 10 N, 20 N, and 30 N, spanning sliding distances of 2000 m and 3000 m to simulate different tribological conditions. Throughout testing, real-time measurements of frictional force and volumetric wear were recorded, enabling precise calculation of wear rates. Data variability was analyzed, and friction coefficient versus sliding distance graphs were plotted. To ensure statistical reliability, triplicate specimens per composition were tested under each condition, with averaged results reported for comprehensive performance assessment.

Figure 8: Wear and friction monitor machine and wear specimen.

RESULTS AND DISCUSSION

Microstructure

Fig. 9 (a) and (b) presents the high-resolution scanning electron microscope (SEM) micrograph of the AA7075 hybrid composite reinforced with 5 wt.% TiB_2 and 4 wt.% ZrO_2. The image reveals detailed microstructural features, including the uniform dispersion of reinforcement phases within the aluminum matrix and the nature of the interfacial bonding, which are critical to understanding the composite's enhanced mechanical and tribological performance. We can see the variation in the number and distribution of reinforcement particles. Ceramic particles appear to have faceted morphology.

Fig. 9 (c) and (d) presents the SEM micrograph of the AA7075 hybrid composite reinforced with 5 wt.% TiB_2 and 6 wt.% ZrO_2. The Inset of Fig. 10 shows that TiB_2 and ZrO_2 ceramic particles exist with an average particle size of 110 ± 0.7 nm. The microstructure reveals the complete uniform distribution of the reinforcement's particles. The resulting structure typically has a fine equiaxed grained and well-ordered microstructure, which is desirable in most casting [4-13]. Notably, these particles tend to localize predominantly along grain boundaries, displaying pronounced agglomeration within the matrix. Insets in Figs. 9 and 10 further illustrate the heterogeneous distribution of the reinforcement phases, indicating particle clustering that intensifies with the elevated weight fraction of reinforcements. This phenomenon is attributed to the increased surface energy of the ceramic particles, which promotes aggregation and challenges uniform dispersion at higher loadings [14].

AA7075/5%TiB_2/2%ZrO_2 hybrid composite resulted in the low mechanical properties obtained from the SEM and mechanical tests conducted. The results are not satisfactory when compared with the 4% ZrO_2 system, even though there is less agglomeration of reinforced particles. A lower percentage of the metal matrix may have resulted in low mechanical properties. The solidification front significantly impacts the displacement of the reinforcements in the casting process. In the process of solidification, the liquid metal moves towards the cooling front, while the reinforcements experience forces like drag and shear force from the molten metal. The distribution of reinforcing particles in intra and intergranular areas determines the velocity of the solidification front. When the solidification front's rate falls below a critical velocity in the process of attaining an equilibrium state, the system may maintain a stable or orderly solidification, which can be inferred from Fig. 10 (a) for AA7075/5%TiB_2/4%ZrO_2 hybrid composite system. When the solidification front's velocity is above the critical velocity, the system may transition to an unstable regime. The reinforcement particles migrate towards the mold walls or get trapped in certain regions depending on the cooling rate, nature, and amount of the reinforcements while

achieving the equilibrium state, leading to agglomeration or mushy zones as inferred in Fig. 10(b) for AA7075/5%TiB_2/6%ZrO_2 hybrid composite system.

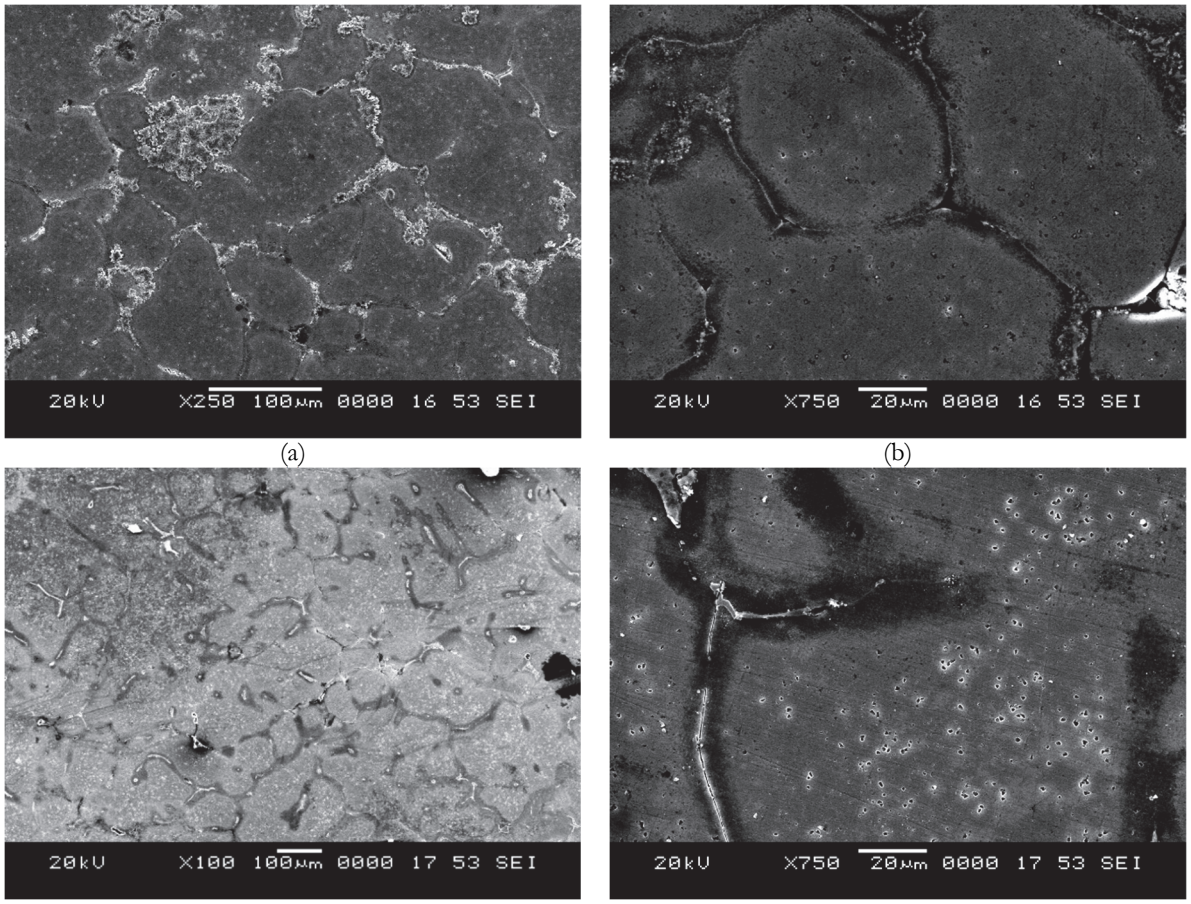

(a) (b) (c) (d)

Figure 9: SEM micrographs illustrating the microstructural morphology of AA7075 metal matrix composites reinforced with TiB_2 and ZrO_2: (A) Composite containing 5 wt.% TiB_2 and 4 wt.% ZrO_2, highlighting the homogeneous dispersion and interfacial bonding of ceramic particulates within the aluminum matrix; (B) Magnified view of the same composition emphasizing particle distribution and matrix–reinforcement interactions. C) Hybrid composite containing 5 wt.% TiB_2 and 6 wt.% ZrO_2, highlighting particle agglomeration and distribution patterns; (D) High-magnification view of the same composition illustrating interfacial bonding and reinforcement morphology within the aluminum matrix.

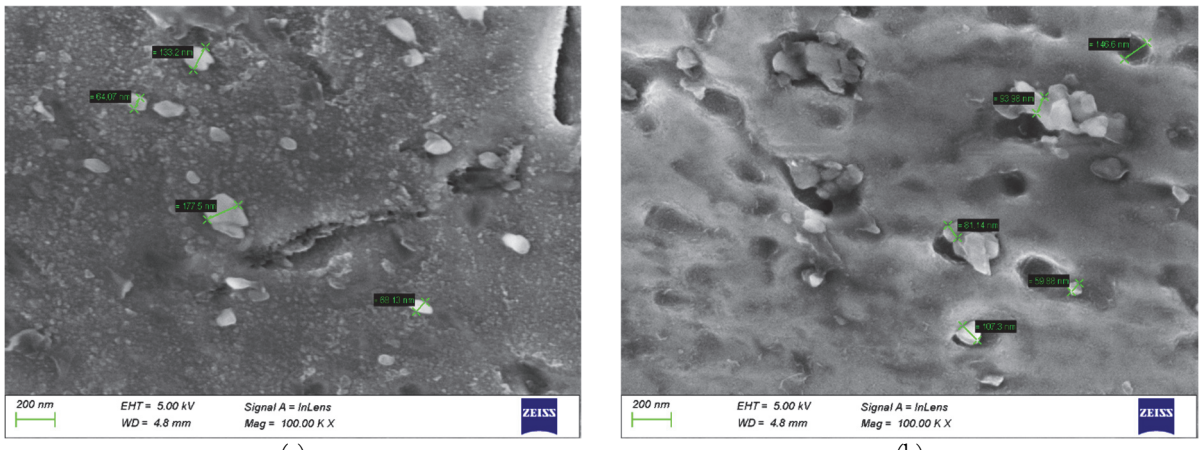

(a) (b)

Figure 10: Particle size distribution analysis of AA7075/TiB_2/ZrO_2 hybrid composites: (A) Composite reinforced with 5 wt.% TiB_2 and 4 wt.% ZrO_2, illustrating nanoscale dispersion; (B) Composite containing 5 wt.% TiB_2 and 6 wt.% ZrO_2, highlighting the impact of increased zirconia content on particle agglomeration and size variation.

Fig. 11 presents the elemental distribution maps obtained via scanning electron microscopy (SEM) for the AA7075/5 wt.% TiB_2/4 wt.% ZrO_2 hybrid composite. The elemental mapping elucidates the spatial dispersion of constituent elements within the composite microstructure. Predominantly, aluminum (Al) forms the matrix, while zinc (Zn) is observed as the principal alloying element. The ceramic reinforcements, represented by titanium (Ti), zirconium (Zr), and boron (B), exhibit a homogenous distribution throughout the matrix without notable agglomeration. This uniform dispersion of reinforcements is critical, as it correlates strongly with enhanced load transfer efficiency and resultant mechanical property improvements, including strength and wear resistance [15, 4].

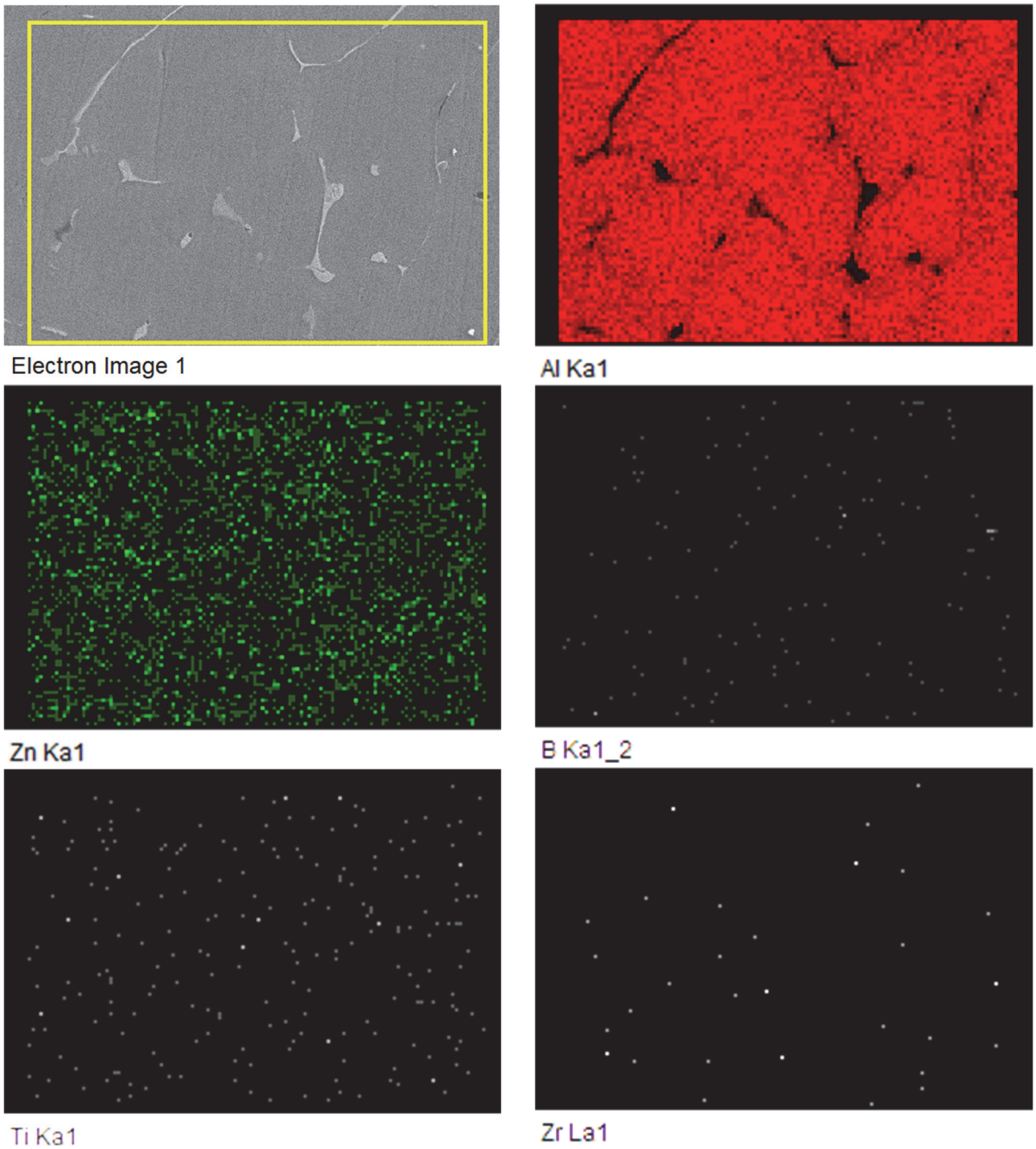

Figure 11: The EDX elemental mapping of AA7075/5%TiB_2/4%ZrO_2.

THE MECHANICAL BEHAVIOUR OF THE COMPOSITES

This section will present the results and discuss the mechanical and physical properties of AA7075/TiB_2/ZrO_2 hybrid composite fabricated through situ casting.

Hardness of the composites

A hardness test was conducted using a Vickers hardness tester. The test specimens were prepared as described in section 2. Three samples, each with a different reinforcement composition, were tested. To ensure accuracy, more than three readings were taken for each specimen, and the average value of 'D' was calculated. Tab. 2 provides a comparison of the hardness between the base matrix AA7075 and the hybrid composites.

Sl. No	Composition (wt. %)	Load (kgf)	Dwell Time (s)	Average 'D' (mm)	Vickers Hardness (Hv)
1	AA7075	-	-	-	55 [16]
2	AA7075/5% TiB_2/2%ZrO_2	10	10	0.4328	98.98±5.26 [17]
3	AA7075/5% TiB_2/4%ZrO_2	10	10	0.4263	102.04±5.72 [17]
5	AA7075/5% TiB_2/6%ZrO_2	10	10	0.449	92.24±5.38 [17]

Table 2: Vickers Hardness values.

It is inferred from Tab. 2 that, first, the hardness increases gradually, and then suddenly, there is a fall in the hardness value. The reinforcements (TiB_2 and ZrO_2) render the inherent property of the matrix material. The literature shows that the best results were obtained for 5wt.% TiB_2 reinforced composite and similarly 4 wt.% ZrO_2 reinforced composite [18]. It was found that adding 5wt% TiB_2 and 2wt% ZrO_2 to the metal matrix increased the hardness value by 80% more than that of the as-cast alloy. By adding 5wt% TiB_2 and 4wt% ZrO_2 to the metal matrix, the hardness value increased by 85.45% compared to as-cast alloy, and similarly, by adding 5 wt.% TiB_2 and 6 wt.% ZrO_2 to the metal matrix, the hardness value increased by 67% more than that of as-cats alloy. As the total weight percentage of the reinforcements increases from 7% (5% TiB_2, 2% ZrO_2) to 9% (5% TiB_2, 4% ZrO_2), there is an increase in the resistance to the dislocation of the particles against the localized deformation. As soon as the total weight percentage of the reinforcements exceeds 9%, resistance to the dislocation is decreased against the load. As per the Hall-Petch theory, grain size refinement increases the area of grain boundaries, which enhances resistance to particle dislocations, thereby improving the composite's hardness. There is an enhancement in the load transfer effect by adding the reinforcement particles, thus enhancing the hardness. [4, 13, 19]

The enhanced dispersion of reinforcement particles within the metal matrix significantly minimizes particle segregation in the AA7075/5 wt.% TiB_2/2 wt.% ZrO_2 and AA7075/5 wt.% TiB_2/4 wt.% ZrO_2 hybrid composites. Notably, the AA7075/5 wt.% TiB_2/4 wt.% ZrO_2 composite exhibits a homogeneous distribution of ceramic reinforcements, as evidenced in Fig. 9, with clearly defined equiaxed grains and well-demarcated grain boundaries. This uniform microstructural morphology mitigates particle agglomeration, thereby contributing to a marked enhancement in hardness values. Conversely, the AA7075/5 wt.% TiB_2/6 wt.% ZrO_2 hybrid composite demonstrates a decline in hardness, attributed to uneven particle dispersion and pronounced agglomeration phenomena, which adversely affect load transfer efficiency and matrix-reinforcement interfacial bonding [20].

Tensile test results

The yield strength (YS), ultimate tensile strength (UTS), and ductility (expressed as percentage elongation) were quantitatively derived from the load-displacement data, subsequently converted into engineering stress-strain parameters. Fig. 12 illustrates the representative stress-strain curves for the AA7075/TiB_2/ZrO_2 hybrid composites, highlighting the influence of varied reinforcement fractions on the composite's mechanical response. These curves provide critical insights into the elastic-plastic deformation behavior, strain hardening characteristics, and fracture mechanisms inherent to the synthesized hybrid metal matrix composites.

The baseline yield strength of the as-cast AA7075 alloy is approximately 107 MPa [16]. Incorporation of 5 wt.% TiB_2 alongside 2 wt.% ZrO_2 into the aluminum matrix resulted in a significant enhancement of yield strength to 113 MPa. Further augmentation of the ZrO_2 reinforcement content to 4 wt.% elevated the yield strength to 123 MPa, indicating an optimal reinforcement threshold for load-bearing capacity. However, a marginal decline to 110 MPa was observed when the ZrO_2

content increased to 6 wt.%, suggesting possible particle agglomeration or stress concentration effects at higher reinforcement fractions.

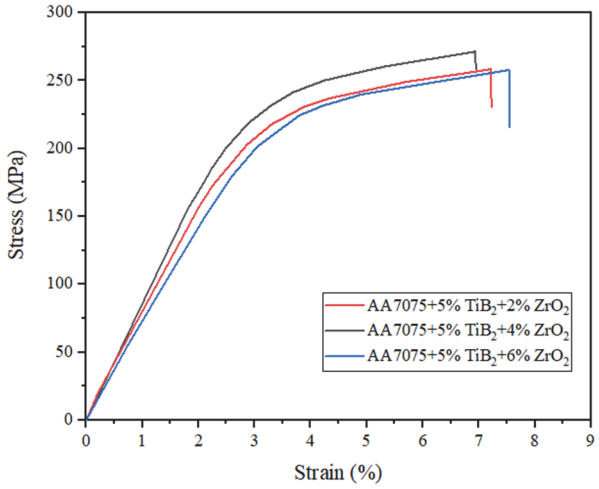

Figure 12: Stress-strain curves for AA7075/TiB_2/ZrO_2 hybrid composites.

Fig. 13 illustrates the variation in yield strength, ultimate tensile strength, and percentage elongation for AA7075/TiB_2/ZrO_2 hybrid composites with varying reinforcement compositions. The composite containing 5 wt.% TiB_2 and 4 wt.% ZrO_2 exhibits the lowest ductility, with elongation reduced to approximately 11%, attributable to its markedly enhanced hardness relative to the as-cast alloy. Across all hybrid composites, a pronounced reduction in ductility is observed, correlating with significant hardness improvements. This inverse relationship highlights the classical trade-off between strength and ductility in particulate-reinforced metal matrix composites. The decreased ductility is primarily ascribed to the reduced inter-particle spacing, which impedes dislocation motion and limits plastic deformation. Under applied loading, the strong interfacial bonding between ceramic reinforcement particles and the AA7075 matrix effectively obstructs dislocation glide and crack propagation, thereby augmenting tensile strength but concurrently restricting elongation. These microstructural interactions underscore the composite's enhanced mechanical robustness and fracture resistance [4, 13].

The AA7075/5 wt.% TiB_2/4 wt.% ZrO_2 hybrid composite exhibits superior yield strength relative to other compositions. This enhancement is primarily attributed to the uniform dispersion of TiB_2 and ZrO_2 ceramic reinforcements within the aluminum matrix and the strong interfacial bonding achieved between the reinforcements and the matrix phase. Across all compositions, the incorporation of TiB_2 and ZrO_2 significantly enhances the interfacial integrity and mechanical anchorage, thereby improving the composite's resistance to reinforcement-matrix debonding under applied stress.

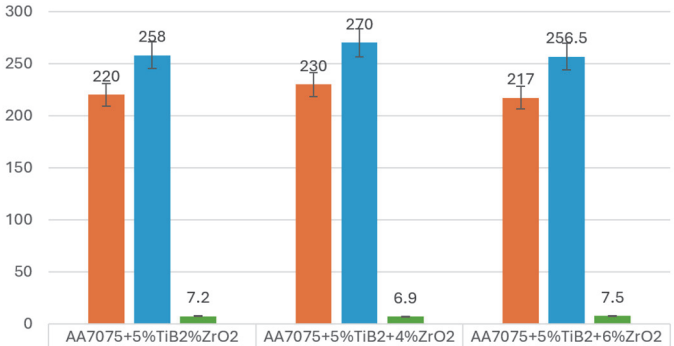

	AA7075+5%TiB2%ZrO2	AA7075+5%TiB2+4%ZrO2	AA7075+5%TiB2+6%ZrO2
Yield Strength (MPa)	220	230	217
Ultimate Tensile Strength (MPa)	258	270	256.5
Elongation (%)	7.2	6.9	7.5

Figure 13: Comparative analysis of yield strength, ultimate tensile strength, and elongation percentage in AA7075-based hybrid composites reinforced with TiB_2 and ZrO_2, demonstrating the influence of reinforcement composition on the mechanical performance and ductility of the material.

TRIBOLOGICAL STUDIES

Dry wear and friction tests were conducted on the wear and friction monitor. The literature states that AMCs are known for superior wear resistance to monolithic aluminum alloys. The mechanical and wear resistance behavior of the hybrid composite increases significantly with the addition of ceramic reinforcements, TiB_2 and ZrO_2, as reported in the literature [4,12,15]. Initially, the volume loss is transient against the sliding distance and attains a steady state after a specific time. In the steady-state wear regime, the wear volume loss is constant for an extended duration.

Fig. 14 illustrates the wear rate behavior of AA7075/TiB_2/ZrO_2 hybrid composites under varying normal loads and sliding distances. An increase in applied load leads to a corresponding escalation in wear rate for each reinforcement composition, indicating a load-sensitive wear mechanism. Similarly, as depicted in Figs. 15 and 16, a progressive increase in sliding distance results in a marked rise in wear rate across all specimens. These observations affirm that both normal load and sliding distance exhibit a directly proportional relationship with wear degradation, attributable to enhanced surface interaction, material removal, and potential thermal softening under prolonged frictional exposure.

The incorporation of ceramic reinforcements in varying weight fractions into the AA7075 aluminum matrix significantly enhances its wear resistance by impeding the extent of plastic deformation within the matrix during tribological interactions. The presence of TiB_2 and ZrO_2 particulates introduces strong barriers to dislocation motion, thereby contributing to improved structural stability and reduced material loss under sliding conditions.

As the sliding distance increases, friction-induced interfacial heating elevates the surface temperature, driving the material closer to a thermally softened, plastically deformable state. This facilitates greater material removal, thereby increasing the wear rate [4, 13]. Among the studied composites, the AA7075/5 wt.% TiB_2/4 wt.% ZrO_2 formulation demonstrates superior wear resistance, primarily attributed to the refined dispersion and homogeneity of the reinforcement phase.

In contrast, the AA7075/5 wt.% TiB_2/6 wt.% ZrO_2 composite exhibits a comparatively higher wear rate, as noted in the inset of Fig. 14. This behavior is linked to non-uniform dispersion and agglomeration of reinforcement particles, as confirmed by the microstructural features in Fig. 17. The clustering of ceramic particulates reduces the effective load transfer efficiency and creates stress concentration zones, thus accelerating wear.

Furthermore, all hybrid composites consistently display lower wear rates compared to the unreinforced AA7075 alloy. This reduction is primarily due to the solid lubricating effect of ceramic particulates under dry sliding conditions, which act as load-bearing constituents and minimize direct metal-to-metal contact. The synergistic strengthening mechanisms—dislocation-particle interactions and robust interfacial bonding—enhance the hardness and tribological stability of the composites, effectively reducing wear-induced damage [21-23].

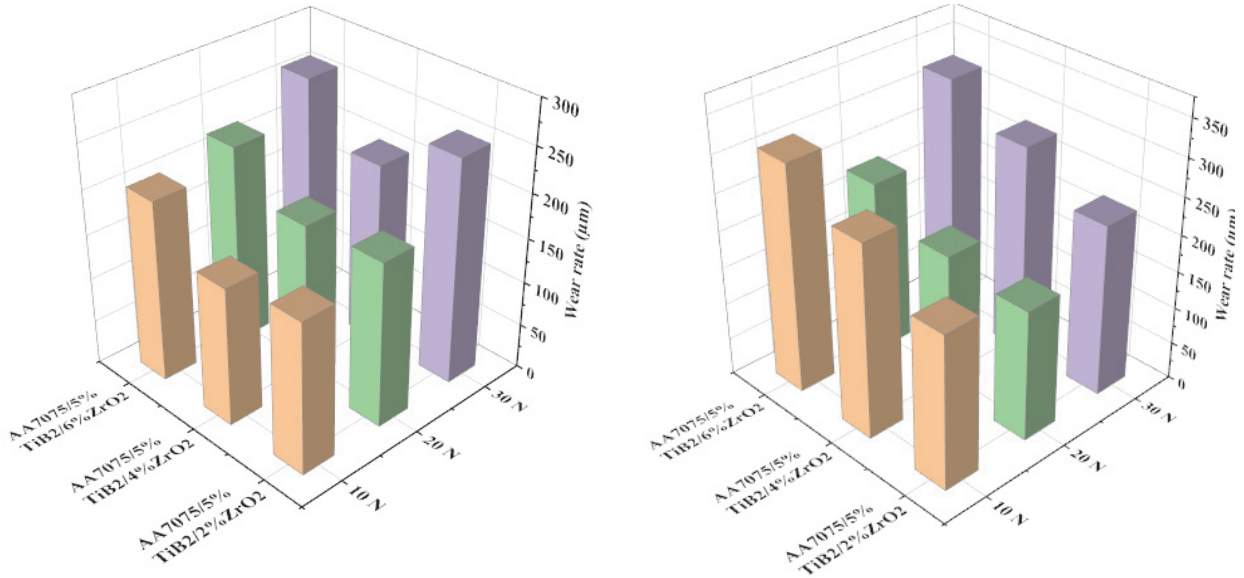

Sliding distance = 2000 m Sliding distance = 3000 m

Figure 14: 3D graph of Wear rate (μm) Vs. Load (N) for different compositions at 2000 m and 3000 m sliding distance.

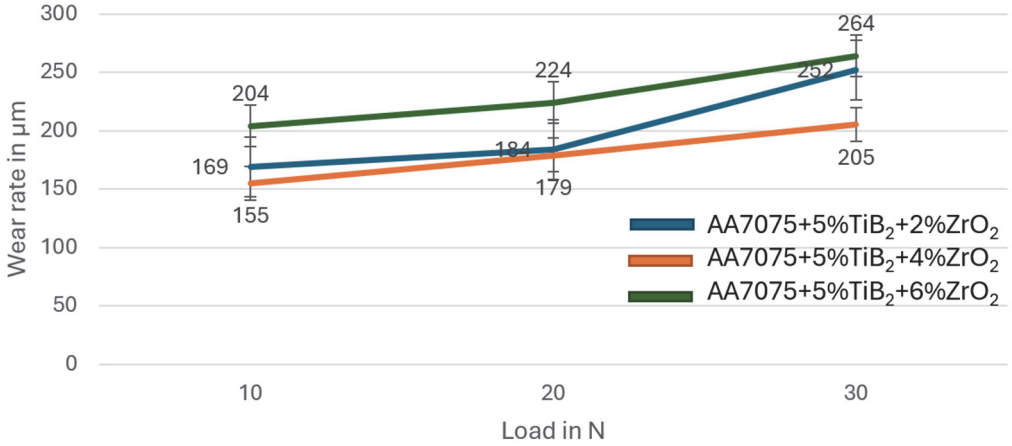

Figure 15: Wear rate Vs. Load for a constant sliding distance of 2000m.

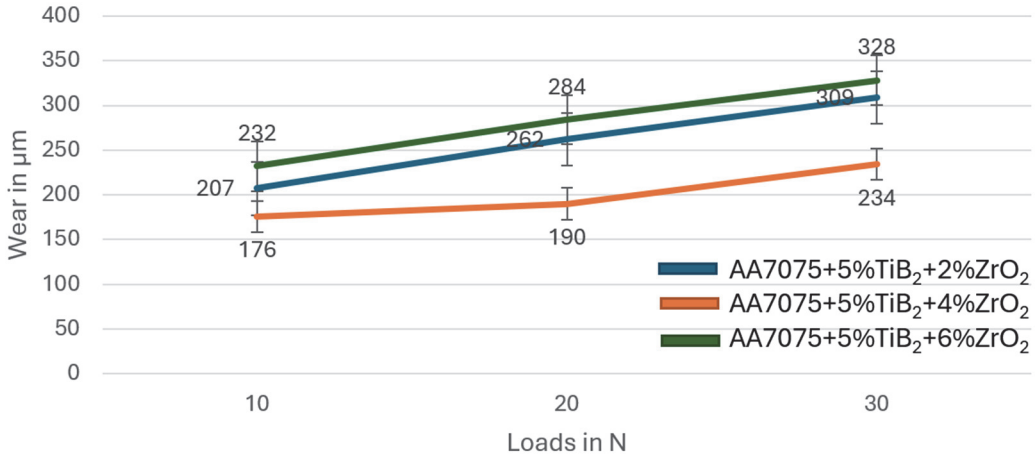

Figure 16: Wear rate vs. Load for a constant sliding distance of 3000m.

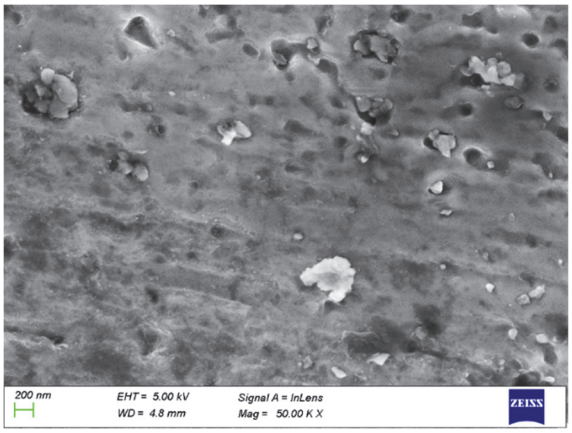

Figure 17: 5 wt% TiB_2 and 6 wt% ZrO_2-Under high magnification stating Agglomeration of reinforced particles.

ANALYSIS OF WORN-OUT SURFACE

Figs. 18, 19, and 20 present scanning electron microscope (SEM) micrographs depicting the worn surface morphologies of AA7075 hybrid composites reinforced with varying weight fractions of TiB_2 and ZrO_2 particles. The intrinsic high hardness of AA7075 alloy imparts substantial resistance against plastic deformation within the

surface layers during wear. Incorporation of TiB_2 and ZrO_2 reinforcements within the aluminum matrix effectively impedes dislocation mobility and shear deformation mechanisms, thereby significantly enhancing the composite's tribological performance and wear resistance. The micrographs show that the grooves are oriented parallel to the wear direction. Due to resistance to plastic deformation, heat develops due to friction. As the surface starts to wear, the load applied and heat generated act as an aid to cause adhesion, which results in micro-joint formation. The groves are parallel to the direction of the wear, and the pattern seems to be ploughing out the surface from the material, which gives evidence of two-body abrasion. Cracks, cavities, and pits are not visible in AA70705/5% TiB_2/4% ZrO_2 and AA7075/5% TiB_2/6% ZrO_2 except in the case of. This may be attributed to the processing quality of AA7075 hybrid composite having 5wt% TiB_2 and 4wt% ZrO_2 and 5wt% TiB_2 and 4wt% ZrO_2 composition. Grooving and scratching appear more severe in AA7075/5% TiB_2/2% ZrO_2, which characterizes the abrasion. Here, the reinforcements TiB_2 and ZrO_2 act as a thin lubricating film between the sliding surface (metal-to-metal contact). Due to this lubricating film, wear resistance has improved [4, 12-25].

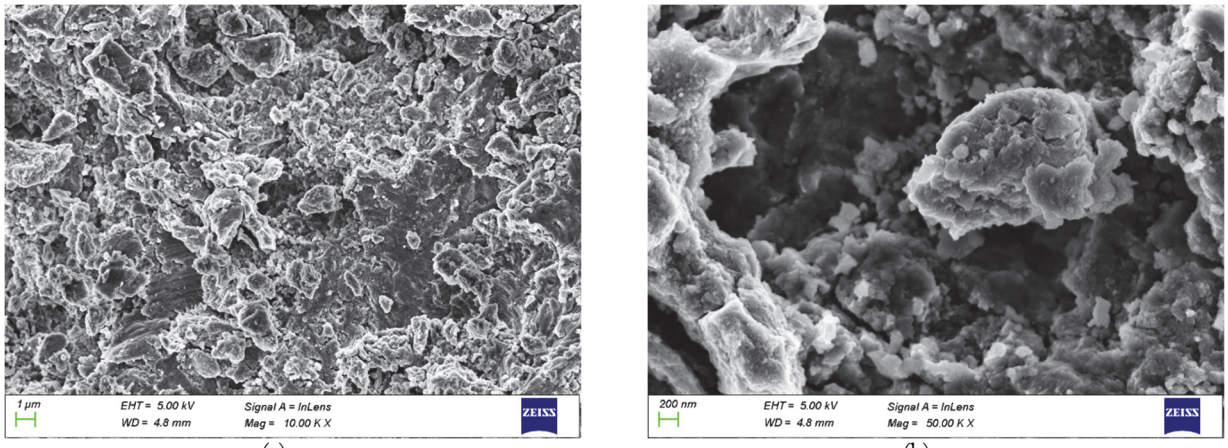

(a) (b)

Figure 18: SEM micrographs illustrating the worn surface morphology of AA7075/TiB_2/ZrO_2 hybrid composites: (a) Composite reinforced with 5 wt.% TiB_2 and 2 wt.% ZrO_2, showcasing wear features at standard magnification. (b) Corresponding high-magnification image revealing detailed microstructural wear mechanisms and particle-matrix interactions for the same composition.

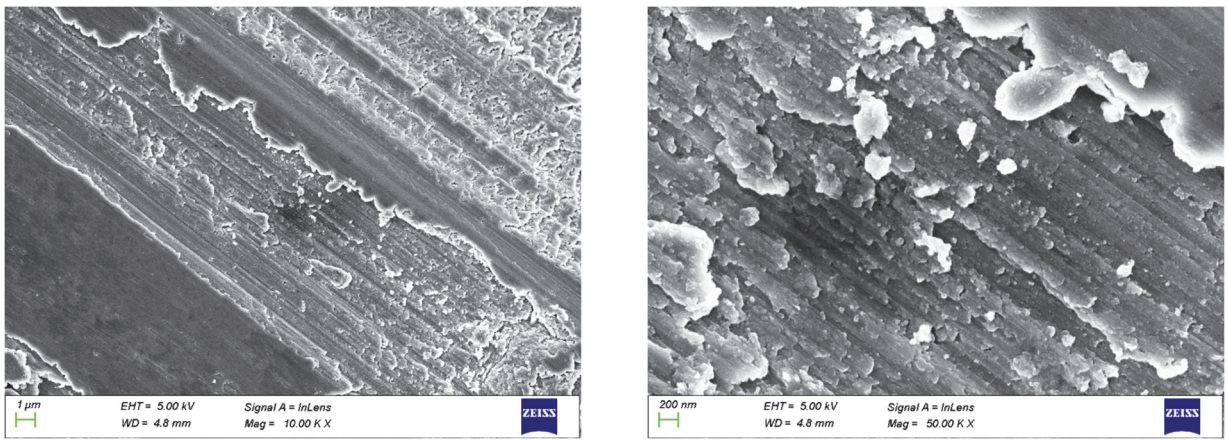

(c) (d)

Figure 19: SEM micrographs depicting the wear morphology of AA7075/TiB_2/ZrO_2 hybrid composite: (c) Surface topography of composite reinforced with 5 wt.% TiB_2 and 4 wt.% ZrO_2 at standard magnification, illustrating wear patterns and material degradation. (d) High-resolution micrograph of the same composition highlighting detailed microstructural features, including wear-induced deformation and particle-matrix interfacial characteristics.

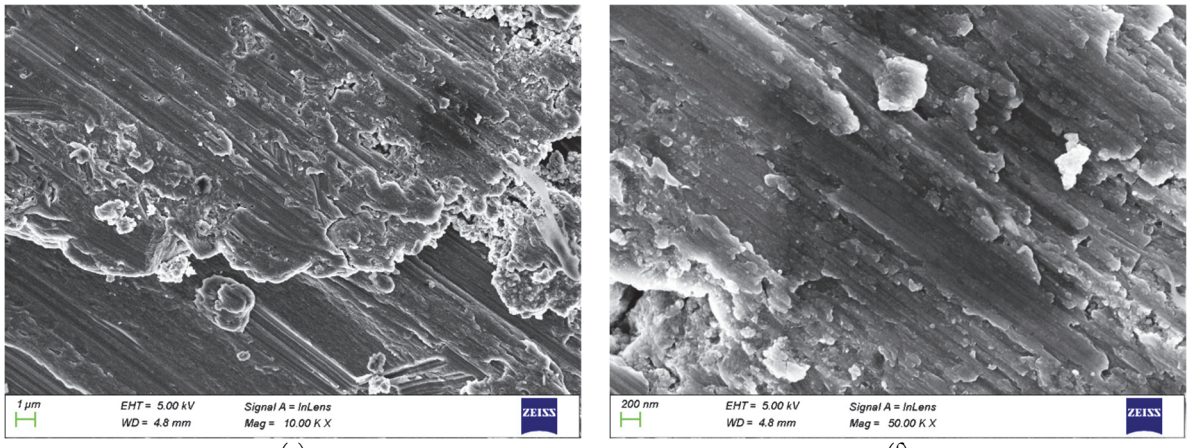

(e) (f)

Figure 20: SEM micrographs illustrating the worn surface morphology of AA7075/TiB_2/ZrO_2 hybrid composite: (e) Composite containing 5 wt.% TiB_2 and 6 wt.% ZrO_2, revealing wear features at standard magnification. (f) High-magnification image of the same composite, detailing microstructural deformation, particle distribution, and wear mechanisms.

EDS SPECTRUM ANALYSIS OF WORN SURFACES

Figs. 21, 22, and 23 illustrate the Energy Dispersive X-ray Spectroscopy (EDS) elemental mapping of the worn surfaces of AA7075 hybrid composites reinforced with varying concentrations of TiB_2 and ZrO_2 particles. The EDS spectra confirm the elemental composition, revealing the presence of aluminum (Al), zinc (Zn), iron (Fe), oxygen (O), boron (B), zirconium (Zr), and titanium (Ti), as detailed in Tab. 3. Prolonged sliding contact induces severe surface deformation, resulting in delamination and the subsequent development of a protective oxide layer on the worn regions, which plays a crucial role in mitigating further material degradation. There is an increase in the temperature in between the rotating disc and wear specimen due to dislocations of the surface by shear force. The worn surface which has undergone large plastic deformation is further exposed to the environment. The active ions on the metal surface due to high temperature rise leads to oxidation. A protective oxide layer is formed around the material may reduce the rate of corrosion which also acts as a lubricant, reducing the wear rate. The presence of oxygen in the EDS spectrum confirms the development of this oxide layer on the worn surfaces. There is the presence of Fe in the spectrum graph as the result of mechanically mixed layer (MML) formation due to rubbing action between the disc and hybrid composite surface [4, 25].

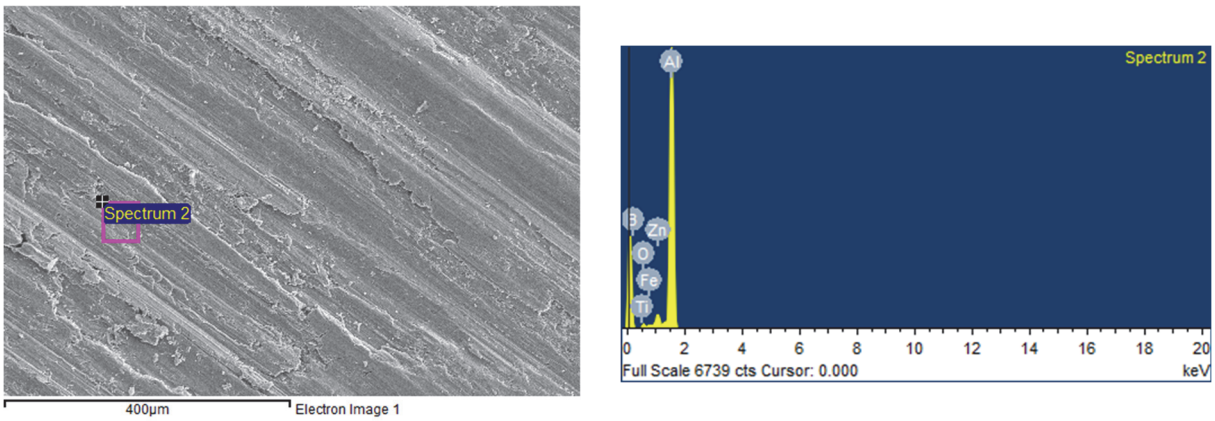

Figure 21: EDS analysis of the worn surface of AA7075/5%TiB_2/2%ZrO_2 hybrid composite.

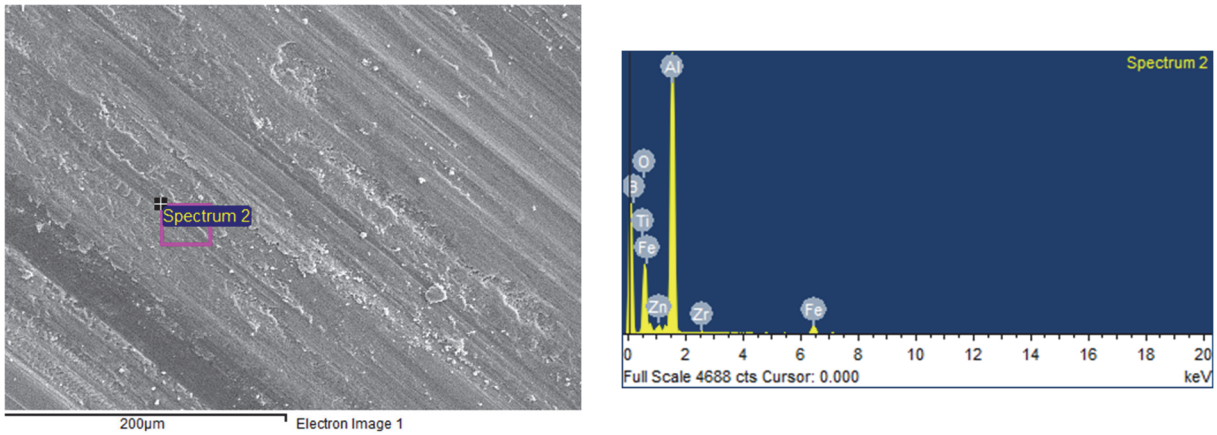

Figure 22: EDS analysis of the worn surface of AA7075/5%TiB_2/4%ZrO_2 hybrid composite.

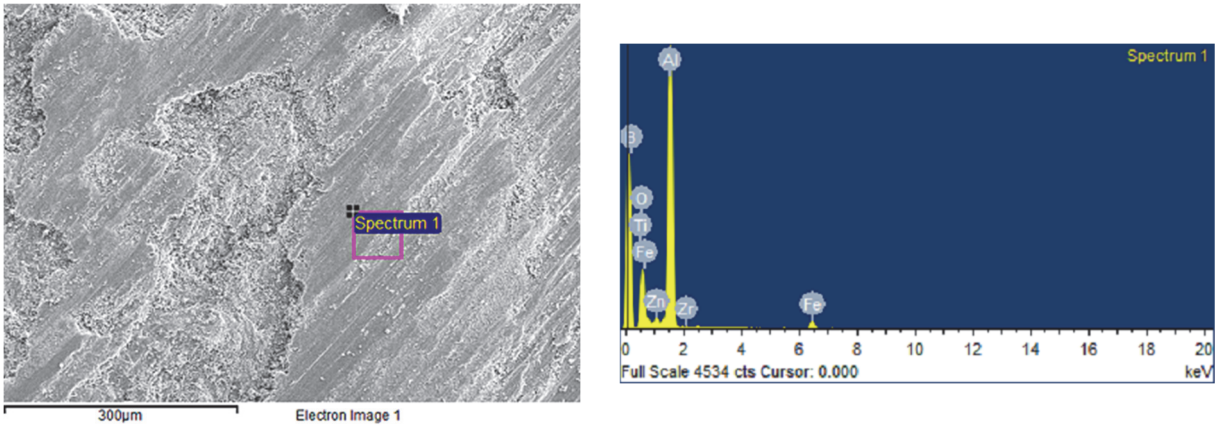

Figure 23: EDS analysis of the worn surface of AA7075/5%TiB_2/6%ZrO_2 hybrid composite.

Composition (wt%)	Elements found in EDS analysis
AA7075/5% TiB_2/2% ZrO_2	Al, Zn, Fe, O, B, Zr and Ti
AA7075/5% TiB_2/4% ZrO_2	Al, Zn, Fe, O, B, Zr and Ti
AA7075/5% TiB_2/6% ZrO_2	Al, Zn, Fe, O, B, Zr and Ti

Table 3: Elements identified in EDS analysis.

CONCLUSIONS

Based on the analysis of microstructural features, mechanical performance, and tribological behavior of AA7075/TiB_2/ZrO_2 hybrid composites fabricated via in-situ casting, the following key conclusions can be drawn:

- A significant enhancement in hardness was observed in all hybrid composites compared to the unreinforced AA7075 alloy. This improvement is primarily attributed to the uniform dispersion of TiB_2 and ZrO_2 particles within the matrix, which promotes grain refinement and impedes dislocation movement. Notably, the AA7075 composite reinforced with 5 wt% TiB_2 and 4 wt% ZrO_2 exhibited the highest hardness increase of approximately 85.45%, followed by 80% for the 5% TiB_2–2% ZrO_2 composite and 67% for the 5% TiB_2–6% ZrO_2 combination. The superior hardness in the 5% TiB_2–4% ZrO_2 composite is linked to its uniform reinforcement distribution and fine-grained structure.
- Microstructural examination revealed equiaxed grain morphology and a homogenous distribution of reinforcements in the 5% TiB_2–4% ZrO_2 composite. However, higher ZrO_2 content (6 wt%) led to visible agglomeration, potentially reducing composite uniformity and performance.

- The integration of TiB_2 and ZrO_2 ceramic reinforcements markedly improved the wear resistance of the AA7075 matrix. Among all compositions, the 5% TiB_2–4% ZrO_2 hybrid composite demonstrated the lowest wear rate, owing to its enhanced hardness and the ability of reinforcements to function as solid lubricants, reducing friction and material loss during sliding contact.
- The yield strength of all hybrid composites with different reinforcement compositions was improved compared to that of the as-cast alloy due to increased resistance to detaining reinforcement particles from the AA7075 matrix. AA7075/5%TiB_2/4%ZrO_2 hybrid composite has higher yield strength than other compositions due to the homogeneous distribution of TiB_2 and ZrO_2 reinforcement particles and good bonding strength between reinforcement particles from the AA7075 matrix.
- Among the various compositions investigated, the AA7075 hybrid composite reinforced with 5 wt% TiB_2 and 4 wt% ZrO_2 demonstrated the most favorable balance of mechanical strength, hardness, and wear resistance, indicating it as the optimal formulation for enhanced performance.
- This investigation has shown the importance of hybrid composites and the beneficial effects of TiB_2 and ZrO_2 ceramic reinforcement particles by adding them to the metal matrix. TiB_2 ceramic reinforcement particles cost around 55.00-60.00 INR (Approx.) for 50 Grams/Grams, and ZrO_2 ceramic reinforcement particles cost about 175.00-180.00 INR (Approx.) for 50 Grams/Grams. In this investigation, various tests were carried out on specimens AA7075/5% TiB_2/2% ZrO_2, AA7075/5% TiB_2/4% ZrO_2, and AA7075/5% TiB_2/6% ZrO_2. The samples were subjected to hardness and wear tests and scanning electron micrographs for microstructural studies.
- Apart from the tests already mentioned, impact and flexural tests can also be conducted to determine the toughness and bending strength.
- Furthermore, hybrid composite can be subjected to ultrasonic treatment (UST) for uniform distribution of reinforcement particles.

ACKNOWLEDGEMENT

The author extends heartfelt appreciation to all individuals and institutions whose invaluable support, guidance, and contributions were instrumental in the successful completion of this research.

REFERENCES

[1] Davis, J. R. (1993). Aluminum and aluminum alloys. ASM international. pp. 351–416. DOI:10.1361/autb2001p351.
[2] Rajan, K., Wallace, W. and Beddoes, J.C., (1982). Microstructural study of a high-strength stress-corrosion resistant 7075 aluminium alloy. Journal of Materials Science, 17, pp. 2817-2824. DOI: https://doi.org/10.1007/BF00644656.
[3] Agrawal, L., Yadav, R. and Sexena, A. (2012). Effect of magnesium content on the mechanical properties of Al-Zn-Mg alloys. International Journal on Emerging Technologies, 3(1), pp. 137-140. DOI: https://doi.org/10.2464/JILM.48.340.
[4] Meti, V.K.V., Shirur, S., Nampoothiri, J., Ravi, K.R. and Siddhalingeshwar, I.G. (2018). Synthesis, characterization and mechanical properties of AA7075 based MMCs reinforced with TiB_2 particles processed through ultrasound assisted in-situ casting technique. Transactions of the Indian Institute of Metals, 71, pp. 841-848. DOI: https://doi.org/10.1007/s12666-017-1216-5.
[5] Meti, V.K., Vishwanath, K.G. and Siddhalingeshwar, I.G. (2017). A review on mechanical and tribological behaviour of aluminum matrix composites processed through liquid state techniques. Indian Foundry Journal, 63(4), pp. 28-47.
[6] Rajan, H.M., Ramabalan, S., Dinaharan, I. and Vijay, S.J. (2013). Synthesis and characterization of in situ formed titanium diboride particulate reinforced AA7075 aluminum alloy cast composites. Materials & Design, 44, pp.438-445. DOI: https://doi.org/10.1016/j.matdes.2012.08.008.
[7] Reddy, M.P., Raju, H.P., Banapurmath, N.R. and Meti, V.K.V. (2022). Influence of ZrO_2 nano particles on the behavior of mechanical and tribological properties of the AA7075 composite. Proceedings of the Institution of Mechanical Engineers, Part N: Journal of Nanomaterials, Nanoengineering and Nanosystems, 236(1-2), pp. 55-62. DOI: https://doi.org/10.1177/2397791420981525.

[8] Zhou, M.Y., Ren, L.B., Fan, L.L., Zhang, Y.W.X., Lu, T.H., Quan, G.F. and Gupta, M. (2020). Progress in research on hybrid metal matrix composites. Journal of Alloys and Compounds, 838, p.155274. DOI: https://doi.org/10.1016/j.jallcom.2020.155274.

[9] Kumar, A., Singh, R.C. and Chaudhary, R. (2020). Recent progress in production of metal matrix composites by stir casting process: An overview. Materials Today: Proceedings, 21, pp.1453-1457. DOI: https://doi.org/10.1016/j.matpr.2019.10.079.

[10] Kumar, P. and Kumar, B. (2024). Effect of T6 heat treatment on mechanical and tribological properties of fabricated AA7075/ZrB_2/Fly ash hybrid aluminum metal matrix composite by ultrasonic-assisted stir casting enroute. International Journal of Metalcasting, 18(3), pp. 2396-2414. DOI: https://doi.org/10.1007/s40962-023-01177-5.

[11] ASM Handbook 1997 Heat Treating. ASM International. Materials Park, OH, USA, 4, pp. 841-887.

[12] Venkatachalam, S., Baskaran, S., Karrthik, R.S., Raj, D.B.T.G. and Kumar, T.R. (2019). Titanium diboride reinforced aluminum composite as a robust material for automobile applications. In AIP Conference Proceedings, 2128(1), p. 020010. DOI: https://doi.org/10.1063/1.5117922.

[13] Meti, V.K.V., Raju, G.U., Siddhalingeshwar, I.G. and Gaitonde, V.N. (2022). Role of Reinforcement Particle Size and Its Dispersion on Room Temperature Dry Sliding Wear of AA7075/TiB_2 Composites. International Journal of Surface Engineering and Interdisciplinary Materials Science (IJSEIMS), 10(1), pp. 1-13. DOI: 10.4018/IJSEIMS.2022010102.

[14] Kumar, D.S. and Suman, K.N. (2021). Wheels in automotive industry—A case study toward the development of magnesium-based composite wheels. In Biocomposite and Synthetic Composites for Automotive Applications, pp. 275-304. Woodhead Publishing. DOI: https://doi.org/10.1016/B978-0-12-820559-4.00011-0.

[15] Bhowmik, A., Dey, D. and Biswas, A. (2021). Comparative study of microstructure, physical and mechanical characterization of SiC/TiB_2 reinforced aluminium matrix composite. Silicon, 13(6), pp. 2003-2010. DOI: https://doi.org/10.1007/s12633-020-00591-2.

[16] Kuldeep, B., Ravikumar, K.P., Pradeep, S. and Gopi, K.R. (2018). Effect of boron nitride and zirconium dioxide on mechanical behavior of Al7075 metal matrix hybrid composite. Materials Research Express, 6(3), p.036509. DOI: https://doi.org/10.1088/2053-1591/aaf36b.

[17] Chikkamath, A.S., Meti, V.K.V. and Siddhalingeshwar, I.G. (2024). Investigating the Synergistic Impact of TiB_2 and ZrO_2 Reinforcements on Forged AA7075-Based Hybrid Metal Matrix Composites. In Materials Science Forum, 1135, pp. 97-111. Trans Tech Publications Ltd. DOI: https://doi.org/10.4028/p-IrH8Mj.

[18] Rathaur, A.S., Katiyar, J.K. and Patel, V.K. (2019). Experimental analysis of mechanical and structural properties of hybrid aluminium (7075) matrix composite using stir casting method. In IOP Conference Series: Materials Science and Engineering 653(1), p. 012033. IOP Publishing. DOI: https://doi.org/10.1088/1757-899X/653/1/012033.

[19] Madhukar, P., Selvaraj, N., Gujjala, R. and Rao, C.S.P. (2019). Production of high performance AA7150-1% SiC nanocomposite by novel fabrication process of ultrasonication assisted stir casting. Ultrasonics Sonochemistry, 58, p.104665. DOI: https://doi.org/10.1016/j.ultsonch.2019.104665.

[20] Sharma, A. and Mishra, P.M. (2019). Effects of various reinforcements on mechanical behavior of AA7075 hybrid composites. Materials Today: Proceedings, 18, pp. 5258-5263. DOI: https://doi.org/10.1016/j.matpr.2019.07.526.

[21] Moustafa, E.B., Melaibari, A. and Basha, M. (2020). Wear and microhardness behaviors of AA7075/SiC-BN hybrid nanocomposite surfaces fabricated by friction stir processing. Ceramics International, 46(10), pp. 16938-16943. DOI: https://doi.org/10.1016/j.ceramint.2020.03.274.

[22] Saravanan, S., Sreenithi, A., Ajitha, M., Ilakkiyal, R., Narmatha, S.R., Rajkumar, S. and Karthikeyan, K. (2020). Tribological behaviour of aluminum alloy (AA7075) based hybrid composites. In IOP Conference Series: Materials Science and Engineering, 923(1), p. 012053. DOI: https://doi.org/10.1088/1757-899X/923/1/012053.

[23] JeFoa, A. (1953). Contact and rubbing of flat surfaces. Journal of applied physics 24(8), pp. 981-988. DOI: https://doi.org/10.1063/1.1721448.

[24] Rabinowicz, E. and Tanner, R.I. (1966). Friction and wear of materials. Journal of Applied Mechanics, 33(2), p.479. DOI: https://doi.org/10.1115/1.3625110.

[25] Stott, F.H. (1998). The role of oxidation in the wear of alloys. Tribology International, 31(1-3), pp. 61-71. DOI: https://doi.org/10.1016/S0301-679X(98)00008-5.